Journal of
Mechanics of
Materials and Structures

◼
◼▪msp
◼

DYNAMICAL CHARACTERIZATION OF MIXED FRACTAL STRUCTURES

Luiz Bevilacqua and Marcelo M. Barros

It is because of people like Marie-Louise and Charles that it is worth fighting for a better world.

We present a new technique to determine the fractal or self-similarity dimension of a sequence of curves. The geometric characterization of the sequence is obtained from the mechanical properties of harmonic oscillators with the same shape of the terms composing the given sequence of curves. The definition of "dynamical dimension" is briefly introduced with the help of simple examples. The theory is proved to be valid for a particular type of curves as those of the Koch family. The method is applied to more complex plane curves obtained by superposing two generators of the Koch family with different fractal dimensions. It is shown that this structure is composed by two series of objects one of which is fractal and the other which is not rigorously a fractal sequence but approaches asymptotically a fractal object. The notion of quasifractal structures is introduced. The results are shown to provide good information about the structure formation. It is shown that the dynamical dimension can identify randomness for certain fractal curves.

1. Introduction

The correlation between the form and the physical properties of certain objects and the fractal characteristics of their geometry has called the attention of several researchers [Feder 1988; Gouyet 1996; Mandelbrot 1982; Mauroy et al. 2004]. However the determination of the geometric fractal dimension of a given sequence of objects using the associated sequence of a selected physical property has not yet been explored as far as we know. In previous papers we have shown that coupling between physics and geometry of fractal objects can be used to determine the fractal dimension of curves belonging to the Koch family.

It was shown that dynamical properties of curves belonging to a fractal sequence can also be fractal. Namely, the periods of a sequence of simple oscillators associated to a given Koch sequence have been successfully used to determine the geometric fractal dimension of the given sequence [Bevilacqua et al. 2008]. We present below the more important results obtained for Koch curves that will help to understand the numerical approach used here to deal with complex curves as explained later on.

We say that a sequence of curves belongs to the Koch family if the k-th order term contains N_k segments with the same length λ_k. The number of segments and the respective lengths are given by $N_k = p^k$ and $\lambda_k = L_0/q^k$ where L_0 is the initial basis or the initiator and p, q are integers. We will use this definition throughout this paper.

Consider a sequence of springs consisting of wires folded in such a way as to reproduce the same geometric shape of the corresponding terms of a given sequence of fractal curves. With these springs is
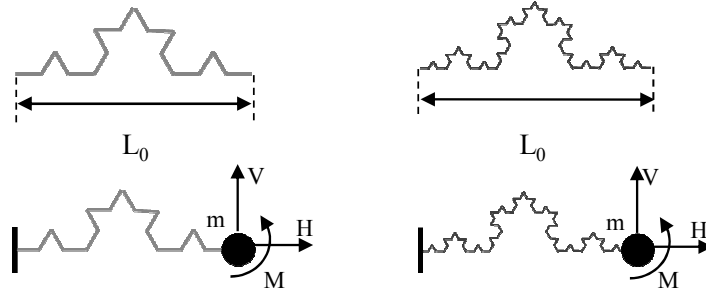
Figure 1. Top: two terms of the fractal geometric sequence. Bottom: Corresponding dynamic oscillators used to characterize the geometric sequence. The mass attached at the extremity of the spring is represented by m.

then possible to construct a simple spring-mass harmonic oscillators sequence by clamping one of the extremities and attaching a mass m at the free extremity. This oscillator sequence as shown in Figure 1 will be called the dynamic characteristic sequence.

It can be shown that it is possible to derive relatively simple relations between the geometric fractal dimension of Koch curves and the fundamental periods of the related harmonic oscillators. Note that the fundamental periods refer to each oscillator as a single isolated spring mass system. That is for a sequence comprising n terms each one defined by the pair (N_k, λ_k) $k = 1, 2, \dots, n$ where N_k and λ_k stand for the number of terms and their lengths respectively there will be n simple harmonic oscillators each one characterized by the corresponding fundamental period T_k^f. The superscript f stays for the respective degree of freedom excited by the initial conditions induced by a horizontal force H, a vertical force V or a moment M. Since N_k can be written as a function of λ_k it is therefore possible to plot the elementary length λ_k against the fundamental frequency T_k^f. Figure 2 illustrates the polygonal curve representing the relation between the logarithm of the normalized variables λ_k/L_0 and T_k^H/T_0^H up to the sixth term for a given Koch sequence corresponding to an initial excitation induced by a horizontal force H.

We claim that the slopes of the segments composing the polygonal curve tend to a fixed value s which is correlated with the fractal dimension D of the Koch sequence. That is $\lim_{k \to \infty} s_k = s$ and consequently
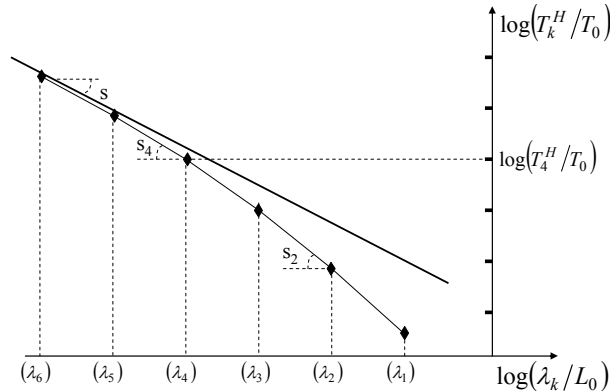
Figure 2. The vertices of the polygonal curve represent the relation between the terms of order k and the normalized frequencies of the corresponding oscillators.
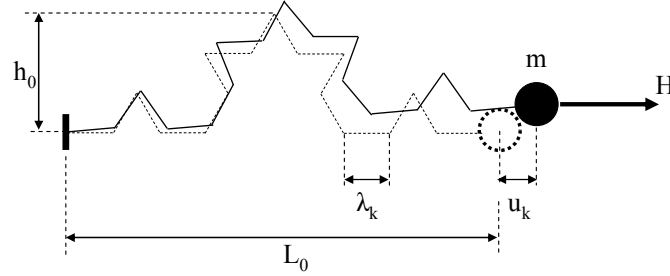
Figure 3. Oscillator corresponding to a term k of the Koch triadic carrying a mass m at the free end and excited by an initial displacement induced by a horizontal force H.

the slope of the last segment in the polygonal curve leads to the fractal dimension of the Koch sequence with increasing precision.

In order to keep this paper as self-contained as possible we will reproduce the proof of the convergence of the slopes s_k to the slope s as $k \to \infty$ or equivalently as $\lambda_k \to 0$.

Consider the Koch triadic sequence. Figure 3 represents the simple oscillator corresponding to a general term k in the sequence.

Let us assume that all the independent oscillators carry an equal mass m at the free end. Imposing an initial displacement generated by a horizontal force H applied at the free end the motion is governed by the elementary equation

$$m \frac{d^2 w_k}{dt^2} + \frac{w_k}{c_{11}^{(k)}} = 0, \tag{1}$$

where w_k is the generalized displacement and $c_{11}^{(k)}$ is the compliance or the inverse of the rigidity. For linear elastic structures the compliance is given by

$$c_{11}^{(k)} = \frac{\partial W_k}{\partial H}\bigg|_{H=1} \tag{2}$$

W_k stands for the stored elastic energy. For the system under consideration the elastic energy stored in a general term k is primarily due to the bending moment distributed along the N_k segments with length λ_k composing the term of order k in the Koch triadic. Therefore the stored bending energy for the k-th order term is

$$W_k = \frac{1}{2} \int_0^{L_t} \frac{M_k^2(s)}{EI} ds = \frac{1}{2} \frac{1}{EI} \sum_{i=0}^{N_k} \int_0^{\lambda_k} (M_{i-1,i}^{(k)}(s))^2 ds, \tag{3}$$

where E is the Young modulus of the wire material and I the moment of inertia of the wire cross section. Both will be assumed constant for all the oscillators. $M_{i-1,i}^{(k)}$ is the bending moment acting on the elementary segment $(i-1, i)$ as shown in Figure 4 and N_k is the total number of segments in the k-th order term. We are disregarding the contribution of the shear and normal forces to the strain energy. Now all the oscillators, for all k, fit into a box $L_0 \times h_0$ as can be seen from Figure 4. The bending moment along a segment $(i-1, i)$ is

$$M_{i-1,i}^{(k)}(s) = H[y_{i-1}^{(k)} + (y_i^{(k)} - y_{i-1}^{(k)})s] \quad \text{where } 0 \leq s \leq 1. \tag{4}$$
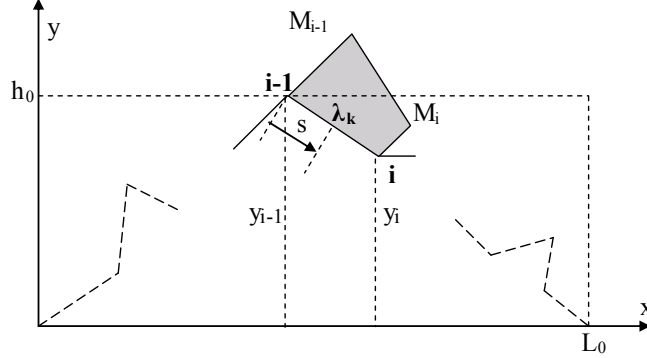
Figure 4. Bending moment along the segment $(i - 1, i)$ for a general term k of the oscillator sequence.

Now introducing (4) into (3), integrating over all segments λ_k and summing up we get

$$W_k = \frac{1}{2} \frac{H^2}{E_k I_k} \lambda_k h_0^2 N_k \Omega_k,$$

where

$$\Omega_k = \frac{1}{N_k} \sum_{i=1}^{N_k} \alpha_i(k)$$

and $\alpha_i(k) = \frac{1}{3}[z_{i-1}^2 + z_{i-1}z_i + z_i^2]$ with $z_j = y_j/h_0$.

From the definition of h_0 clearly $z_j \leq 1$ for all j, and consequently $\alpha_i(k) \leq 1$.

The compliance can now be derived from the stored energy function W_k:

$$c_{11}^{(k)} = \left. \frac{\partial W_k}{\partial H} \right|_{H=1} = \frac{h_0^2}{E_k I_k} N_k \lambda_k \Omega(k). \tag{5}$$

Introducing this expression into (1) we obtain

$$\frac{d^2 u_k}{dt^2} + \frac{1}{(T_k^H)^2} u_k = 0, \tag{6}$$

where the period T_k^H is given by

$$T_k^H = \left(\frac{m h_0^2 L_0}{EI} \frac{\lambda_k}{L_0} N_k \Omega_k \right)^{1/2}. \tag{7}$$

Now from the definitions of N_k and λ_k for curves of the Koch family there comes immediately

$$\log N_k = -\log\left(\frac{\lambda_k}{L_0}\right) \frac{\log p}{\log q}. \tag{8}$$

Introducing the value of N_k given by the equation above into (7) and after some straightforward calculations we obtain

$$\log \frac{T_k^H}{T_0^I} = \frac{1}{2} \log \Omega_k + \frac{1}{2}(1 - D) \log \frac{\lambda_k}{L_0}, \tag{9a}$$

where $D = \log p / \log q$ and T_0^I is a reference period:

$$(T_0^I)^2 = \frac{m_0 h_0^2 L_0}{E_0 I_0}.$$

The parameter D is the dynamical fractal dimension. It coincides with the box and the Hausdorff fractal dimensions provided that the mass, the Young modulus and the diameter of the wire cross section are all constant.

Now, if the geometric fractal dimension of the Koch sequence can be determined through the sequence of the periods of the corresponding oscillators, it is necessary that the (9a) plotted on the plane $Y_k \times X_k$, with $Y_k = \log(T_k/T_0)$ and $X_k = \log(\lambda_k/L_0)$, approaches a straight line whose angular coefficient is equal to $(1 - D)/2$ as shown in Figure 2. Define the functional relation $Y_k \Leftrightarrow X_k$ as a polygonal curve composed by straight segments connecting the points (X_k, Y_k); (X_{k+1}, Y_{k+1}). Let us prove the asymptotic behavior of the polygonal curve. The following lemma is proved in the Appendix.

Lemma. *For curves belonging to the Koch family — class of curves defined by $N_k = p^k$ and $\lambda_k/L_0 = 1/q^k$ — the first order differential form of the quadratic term Ω_k with respect to λ_k is finite for increasing values of k, or equivalently decreasing values of λ_k. That is,*

$$\lim_{k \to \infty} (\Delta\Omega_k/\Delta\lambda_k) = \lim_{\lambda_k \to 0} (\Delta\Omega_k/\Delta\lambda_k)$$

is finite.

Now recalling (9a) and with $Y_k = \log(T_k/T_0)$ and $X_k = \log(\lambda_k/L_0)$ the calculation of the differential ratio $\Delta Y_k/\Delta X_k$ after some simple operations gives

$$\frac{\Delta Y_k}{\Delta X_k} = \frac{1}{2\Omega_k}\frac{\Delta\Omega_k}{\Delta\lambda_k}\lambda_k + \tfrac{1}{2}(1 - D).$$

Therefore from the lemma and since Ω_k is finite and nonzero we have

$$\lim_{\lambda_k \to 0} \frac{\Delta Y_k}{\Delta X_k} = \tfrac{1}{2}(1 - D).$$

Proposition 1. *As $k \to \infty$ the curve given by* (9a) *approaches asymptotically a straight line with slope equal to $(1 - D)/2$.*

It was shown that the oscillation period sequence approaches asymptotically a fractal sequence whose fractal dimension exhibits a simple correlation with the geometric fractal dimension for the case of an excitation induced by a horizontal force. Similarly it can be shown that the sequences corresponding to the other two initial conditions, triggered by a vertical force or a moment, are governed by similar laws, namely

$$\log \frac{T_k^V}{T_0^{II}} = \tfrac{1}{2}\log\Psi_k + \tfrac{1}{2}(1 - D)\log\frac{\lambda_k}{L_0} \tag{9b}$$

for a vertical force and

$$\log \frac{T_k^M}{T_0^{III}} = \tfrac{1}{2}(1 - D)\log\frac{\lambda_k}{L_0} \tag{9c}$$

for a moment.

The parameter D is the fractal dimension of the primordial geometric sequence provided that the mechanical properties of the wires acting as springs are the same for all elements.

Note that for the initial condition induced by a moment the sequence of the normalized periods of the simple oscillators follow exactly a power law. The reason is that for this case the bending moment is the same for all the elementary segments, that is, the strain energy is uniformly distributed along the elements composing the respective curve.

Numerical experiments have clearly shown that the fractal dimension of a generalized Koch curve can be determined by the periods of a related oscillator sequence provided that the wire cross section and Young modulus remain the same for all oscillators. It can be shown that if the mass m at the free end is not constant but proportional to the total curve length, for each oscillator, that is, for the k-th oscillator $m_k = \rho N_k \lambda_k$ the factor multiplying $\log(\lambda_k/L_0)$ in (9a)–(9c) should be $1 - D$ instead of $(1 - D)/2$.

The fractal dimension determined with the method introduce above will be called dynamical fractal dimension irrespectively of the value of the mass, constant or not.

Now suppose we are given just one term, sufficiently large, of a hypothetically fractal sequence. The problem now is to find out if the given sample really belongs to some fractal sequence and if so to determine the respective fractal dimension. Let us call this first curve the reference term. Following the same technique exposed before build a spring-mass system using a folded wire with the same shape as the reference term carrying a mass m at one of the extremities and keeping the other clamped (Figure 5, left). It is possible, as already discussed [Bevilacqua et al. 2008] to find three fundamental frequencies corresponding to three selected excitation introduced by a horizontal force H, a vertical force V and a concentrated moment M.

From the reference term — Figure 5, left — cut a piece off the extremity to obtain a new sample with length $L_{n+1} = bL_n$ where $b < 1$ is the scale factor. This operation may be repeated successively to obtain a sequence of samples. Now to each sample corresponds a simple harmonic oscillator and the corresponding periods for all three types of excitation can be determined. Performing this operation in successive steps (Figure 5) it is possible to find a correlation between the periods and the lengths of the sample projections on the horizontal axis. It is convenient, in order to simplify the calculations, to agree on a constant reduction factor $b = L_m/L_{m-1}$ to cut the successive samples.

Call b_m the variable representing the ratio L_m/L_n where L_m is the length of the horizontal projection of the sample m and L_n is the length of the horizontal projection of the reference term. Therefore we have $b_m = b^m$. For the classical Koch curves it is possible to show that:
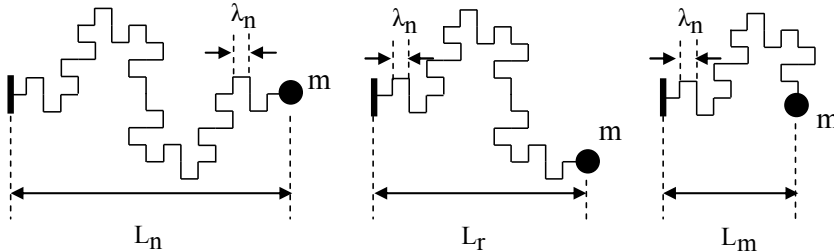
Figure 5. Sequence of three general samples ($m > r > n$) taken from the reference term whose projections on the horizontal axis are L_m, L_r, L_n. The scale b is defined by $L_{r-1} = bL_r$.

(A) For oscillations induced by the action of a concentrated moment:

$$\left(\log \frac{T_{n/m}}{T_n}\right)^{(M)} = \frac{D}{2}\log(b_m) + \Phi_m^{(M)}. \tag{10a}$$

(B) For oscillations induced by the action of a horizontal force or a vertical force we obtain the equations

$$\left(\log \frac{T_{n/m}}{T_n}\right)^{(H)} = \left(1 + \frac{D}{2}\right)\log b_m + \Phi_m^{(H)} \tag{10b}$$

$$\left(\log \frac{T_{n/m}}{T_n}\right)^{(V)} = \left(1 + \frac{D}{2}\right)\log b_m + \Phi_m^{(V)}. \tag{10c}$$

The parameters $\Phi_m^{(M,H,V)}$ in these equation can be interpreted as a kind of noise perturbation intrinsic to the method. The interval of variation of the perturbation $\Phi_m^{(M,H,V)}$ as function of m depends on several conditions other than the scale factor b, as the type of the initial excitation and the geometry of the curves. The analysis of $\Phi_m^{(M,H,V)}$ as a function of m is rather complex even for simple Koch curves. It is possible to show that a first estimation of the relative deviation of the sequence of normalized periods $(T_{n/m}/T_n)$ from the theoretical power law given by $(b_m)^{(1+D/2)}$ is

$$\frac{T_{n/m}/T_n}{(b_m)^{(1+D/2)}} \propto \sqrt{\frac{1-2m\varepsilon_0}{1-mD\varepsilon_0}}, \quad \text{where } \varepsilon_0 = 1 - b > 0.$$

Several numerical experiments were tried for different types of Koch curves. It has been observed that for oscillations induced by a horizontal force the local perturbation is large while for the other two types of excitation induced by vertical force and concentrated moment the noise is very small. In any case the average values obtained with this technique for all boundary conditions are very good particularly for ratios $L_m/L_n > 0.6$.

This paper is intended to show that the dynamical approach is equally applicable for a new class of more complex curves that will be called mixed fractals. Numerical experiments with mixed fractal geometries confirm that the theory developed for Koch curves presents just as good results. In other words, Equations (9a)–(9c) and (10a)–(10c) can be extended to more complex curves.

2. Mixed fractals and quasifractal structures

Figure 6 shows two types of Koch curves C_A and C_B with self-similar or fractal dimensions D_A and D_B respectively. From the definition of Koch curves we may write

$$\log N_k = k \log p$$

and

$$\log \frac{\lambda_k}{L_0} = -k \log q.$$

Eliminating k we obtain

$$\log N_k = -D \log \frac{\lambda_k}{L_0}, \quad \text{where } D = \frac{\log p}{\log q}.$$
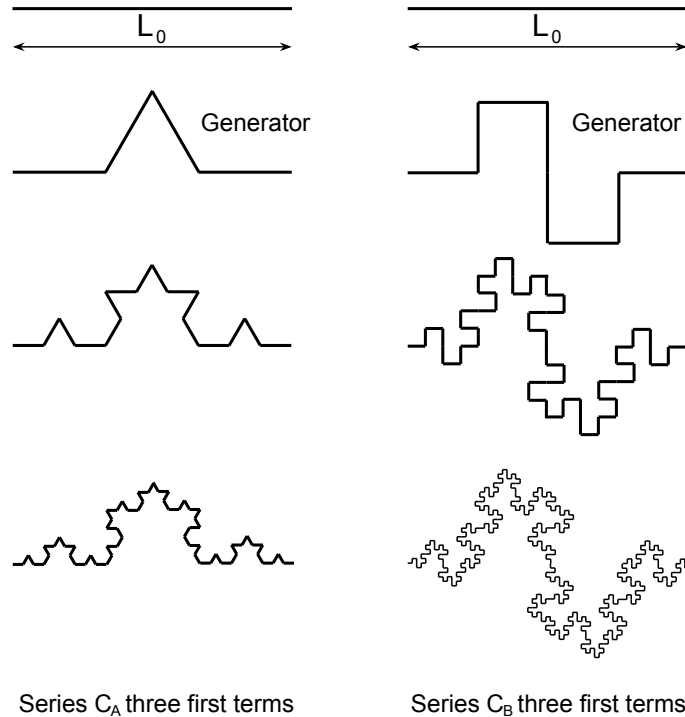
Figure 6. Koch curves C_A and C_B used to generate a new object O. The fractal dimensions are $D_A = \log 4 / \log 3$ and $D_B = 1.5$.

The parameter D is the self-similarity dimension or the fractal dimension. For the Koch triadic C_A and the Koch quadratic C_B, we get $D_A = \log 4 / \log 3 = 1.261859$ and $D_B = \log 8 / \log 4 = 1.5$ respectively.

This paper deals with a series of objects $O : \{O_1, O_2, \ldots, O_n, \ldots\}$ generated with the help of a particular arrangement of two or more curves of the Koch type. We will call this class of objects *mixed fractal curves*. In order to illustrate these ideas let us build a mixed fractal sequence with the help of two particular curves, namely the Koch triadic (C_A) and the Koch quadratic (C_B).

The generation process of a *mixed fractal curve* using the Koch curves C_A and C_B with fractal dimensions D_A and D_B respectively is governed by the following law of formation.

The first term O_1 coincides exactly with the first term, the generator, of the C_A series assembled on a basis with length L_0. That is O_1 consists of $N_1^A = p_A$ segments with length $\lambda_1^A = L_0/q_A$. The second term of the O series is obtained by selecting p_A generators of the series C_B properly scaled such that all of them fit to a basis of length λ_1^A. This means that O_2 consists of $p_A p_B$ segments with length $\lambda_1^B = \lambda_1^A/q_B = L_0/q_A q_B$. The next curves can be obtained repeating the procedure described above, that is by using the elementary segments of the current curve as basis for the following generator of C_A or of C_B properly downscaled. Switching these generators in successive steps all terms of the mixed fractal sequence may be obtained.

Let C_A be the Koch triadic and C_B the Koch quadratic. Taking as initiator the generator of the Koch triadic, ignoring the trivial initiator L_0, the process is simply to switch step by step the generators of both
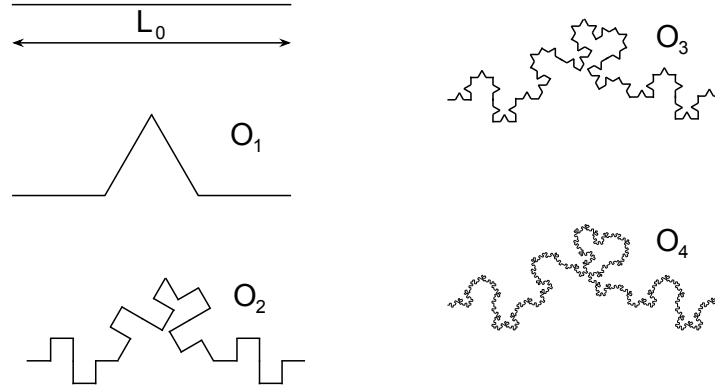
Figure 7. Terms of the series O built up with the Koch curves C_A and C_B.

curves properly scaled to build up a new term of the series O as described above. Figure 7 depicts four terms of the series.

Now, let us investigate the fractal characteristics of this new series built by overlaying alternatively the generators of the triadic and of the quadratic Koch curves on each other properly scaled. Let us assume that the mixed fractal curve belongs to the same class as Koch curves. Then we may write

$$\bar{D}_k = -\frac{\log \bar{N}_k}{\log(\bar{\lambda}_k/L_0)}. \tag{11}$$

If the mixed curve is really a self-similar fractal then $\bar{D}_k$ is independent of k.

Recalling the formation law it is not difficult to calculate the number of segments $\bar{N}_k = (p_A)^i (p_B)^j$ and the segment length $\bar{\lambda}_k = L_0 q_A^{-i} q_B^{-j}$ corresponding to the k-th order term. The integers i and j are either equal or differ by one. That is,

$$\{i, j\} : [i - j = 0 \ \text{ or } \ i - j = 1].$$

Clearly $i + j = k$. This can be expressed analytically by

$$i = \lfloor (k + 1)/2 \rfloor, \quad j = \lfloor k/2 \rfloor,$$

where the $\lfloor \ \rfloor$ indicates the floor function (returning the integer part of a rational number). The expressions for N_k and λ_k can be rewritten using these expressions:

$$\log \bar{N}_k = i \log p_A + j \log p_B \tag{12}$$

and

$$\log(\bar{\lambda}_k/L_0) = -(i \log q_A + j \log q_B). \tag{13}$$

Now using (12) and (13) after some simple operations, the expression (11) becomes

$$\bar{D}_k = \frac{k \log p_A + \lfloor k/2 \rfloor (\log p_B - \log p_A)}{k \log q_A + \lfloor k/2 \rfloor (\log q_B - \log q_A)}. \tag{14}$$

Note that the dimension $\bar{D}_k$ depends on the iteration order k. So it is not possible to say that a mixed curve is fractal, further investigation is necessary. Let us separate the series O into two subsets, the odd series O_{odd} and the even series O_{even}.

For even iterations (14) reads

$$\bar{D}^{\text{even}} = \frac{\log p_A + \log p_B}{\log q_A + \log q_B}. \tag{15}$$

The sequence of even terms has a classical fractal structure with $\bar{D}^{\text{even}}$ independent of k. For odd iterations we have

$$\bar{D}_k^{\text{odd}} = \frac{(k-1)\log p_A + (k-2)\log p_B}{(k-1)\log q_A + (k-2)\log q_B} \quad \text{for } k > 1. \tag{16}$$

Then odd iterations are not strictly fractals. Clearly in the limit, when $k \to \infty$, the expression (16) tends to expression (15) and we may say that the odd sequence approaches asymptotically a fractal sequence. It is remarkable that the series O can be split into two series, O^{even} which is a fractal series and O^{odd} which is not strictly a fractal series, but we could say that it tends to a fractal object when $k \to \infty$. It is possible to generalize the result above to include several fractal curves composing a mixed fractal.

Definition. An infinite set of curves $\{C_1, C_2, \ldots, C_k, \ldots\}$ with the same basis L_0 is said to be a *quasifractal Koch sequence* if, letting $\bar{N}_k$ be the number of segments — all of same length $\bar{\lambda}_k$ — corresponding to the term C_k, the sequence $\{\bar{D}_1, \bar{D}_2, \ldots, \bar{D}_k, \ldots\}$ given by

$$\bar{D}_k = -\frac{\log \bar{N}_k}{\log(\bar{\lambda}_k/L_0)}.$$

satisfies $\bar{D}_i \neq \bar{D}_j$ and has a limit

$$\bar{D} = \lim_{k \to \infty} \bar{D}_k.$$

Suppose that the number of elementary segments and the respective lengths corresponding to a general term C_k are given by

$$\bar{N}_k = p_1^{i_1} p_2^{i_2} \cdots p_m^{i_m} \quad \text{and} \quad (\bar{\lambda}_1/L_0) = q_1^{-i_1} q_2^{-i_2} \cdots q_m^{-i_m} \quad i_1 + i_2 + \cdots + i_m = k,$$

where the pair $(p_j, L_0 q_j^{-1})$ $j = 1, 2, \ldots, m$ corresponds to a simple generator K_j belonging to the Koch family and the exponents i_α are integers function of k, $i_\alpha = f_\alpha(k)$. Then the definition of $\bar{D}_k$ gives

$$\bar{D}_k = \frac{(f_1(k)/f_\beta(k))\log p_1 + (f_2(k)/f_\beta(k))\log p_2 + \cdots + \log p_\beta + \cdots + (f_m(k)/f_\beta(k))\log p_m}{(f_1(k)/f_\beta(k))\log q_1 + (f_2(k)/f_\beta(k))\log q_2 + \cdots + \log q_\beta + \cdots + (f_m(k)/f_\beta(k))\log q_m}.$$

Now if at least one $f_j(k)/f_\beta(k) \neq 1$ and $\lim_{k \to \infty}[f_j(k)/f_\beta(k)] \to 1$ then according to the previous definition the sequence of curves C_k, $k = 1, 2, \ldots, n, \ldots$ is quasifractal. $\square$

According to this definition the odd sequence obtained with the process described above is clearly quasifractal since from (16) we immediately obtain

$$\lim_{k \to \infty} \bar{D}_k^{\text{odd}} = \frac{\log p_A + \log p_B}{\log q_A + \log q_B} = \bar{D}^{\text{even}}.$$
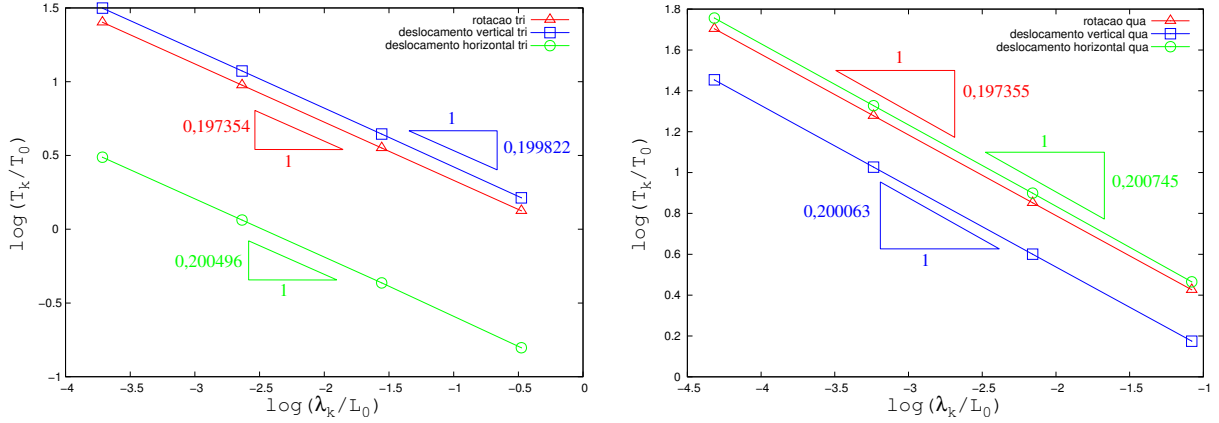
Figure 8. Normalized period $\log T_k/T_0$ versus the normalized length of segments $\log \lambda_k/L_0$ for odd (left) iterations and even (right) iterations of the triadic-quadratic mixed curve.

It is interesting to note that if q_A is close to q_B, that is, if

$$\frac{\log q_B}{\log q_A} = 1 + \varepsilon,$$

the expression (15) can be written as

$$\bar{D}_k^{\text{even}} = \frac{D_A + (1+\varepsilon)D_B}{1 + (1+\varepsilon)}.$$

When $\varepsilon \to 0$ we find that the fractal dimension tends to the mean value

$$\bar{D}_k^{\text{even}} \approx (D_A + D_B)/2.$$

3. Dynamical fractal dimension of mixed fractals

In this section we will use the technique presented in the previous section to investigate the fractal characteristic of the mixed curve presented in the Section 2. The results obtained here, despite the fact that we are dealing with a particular case, suggest that we may expect equally good results for other mixed fractals belonging to the Koch family.

3.1. *Test with a finite subset of consecutive terms removed from a mixed fractal sequence.* Let us test the dynamic fractal dimension method for mixed curves generated by the triadic-quadratic process given the first eight terms. Let eight simple harmonic oscillators be built after the geometry presented in the Figure 7. The eight terms are separated into two sets each one consisting of four terms corresponding respectively to the even sequence and the odd sequence. For the first numerical experiment the oscillators carry a constant mass and are excited by a moment, a horizontal force or a vertical force separately. The results for four terms of each series, the odd series O_{odd} and the even series O_{even} are presented in the Figure 8-a and Figure 8-b. The approximated fractal dimension D_{approx} was obtained with the slope D_{dyn} of the segment joining the points on the graph of Figure 8 corresponding to the two highest order

Exciting force	Mass M_0	Odd iterations		Even iterations	
		D_{dyn}	D_{approx}	D_{dyn}	D_{approx}
Couple	Constant	−0.197354	1.394708	−0.197355	1.394710
Vertical force	Constant	−0.199822	1.399644	−0.200063	1.400126
Horizontal force		−0.200496	1.400992	−0.200745	1.401490
Couple	Variable	−0.394709	1.394709	−0.394711	1.394711
Vertical force	Variable	−0.397130	1.397130	−0.395132	1.395132
Horizontal force		−0.398592	1.398592	−0.398576	1.398576

Table 1. Characterization using four terms of each sequence. Dynamic fractal dimension of odd and even iterations for the mixed triadic-quadratic Koch. Results for two distinct assemblages: constant mass and variable mass proportional to the curve length.

terms in the sequence. According to the theoretical predictions (9a)–(9c), those slopes should relate with the geometric fractal dimension as $D_{\mathrm{approx}} = 1 - 2D_{\mathrm{dyn}}$. The results are displayed on the Table 1 and agree satisfactorily with the correct value of the geometric fractal dimension given by (15). Note that the approximation of the fractal dimension for the odd sequence is indistinguishable from the approximation for the even fractal sequence for practical proposes.

The results for a second numerical experiment with variable mass proportional to the total spring length of the corresponding geometric term are also presented in the Table 1. For this case the fractal geometric dimension expected from the theoretical results should be related to the dynamical fractal dimension according to $D_{\mathrm{approx}} = 1 - D_{\mathrm{dyn}}$ as stated before.

It is important to mention that the oscillator periods were calculated taking into account only the elastic energy stored by the bending moment, disregarding shear and normal forces. The fractal dimension relative to the even iterations is $\bar{D}_0^{\mathrm{even}} = 1.39471$ independent of k. As shown in the Table 1, the deviation from this value is not more than 1.5%. The results are very consistent. It is also interesting to notice that the results for the odd iterations are quite satisfactory if we think of the limit value as $k \to \infty$. The numerical experiment corroborate the conjecture that the technique that has proved to work out for regular Koch curves are also efficient to calculate the dynamical fractal dimension for mixed fractal objects. We believe that this approach opens up a very rich topic for both theoretical and numerical investigation.

3.2. *Test with a single term removed from the mixed fractal sequence.* For this identification problem just one term of the reference sequence is given to find out the respective fractal dimension. Let us take the eighth order term of the Koch triadic-quadratic mixed fractal series. The projection of this curve on the horizontal axis is therefore equal to the initiator length, that is $L_n = L_0$. Figure 6 shows how the normalized periods for 14 samples obtained from the reference curve as explained in the introduction varies with respect to the successive length ratios. The cuts were made following a rather large scale $b = 1/2$ reducing each sample successively according to the rate $L_k = (L_{k-1})/2$.

Figure 9 shows the normalized periods versus the sample lengths for the three excitation types. The Table 2 shows the slope D_{dyn} of interpolated straight lines corresponding to the points on the figure representing the three excitation types and the derived approximated fractal dimension D_{approx}. According to the theoretical prediction (9a)–(9c), the relations between the geometric fractal dimension and the

Exciting force	D_{dyn}	D_{approx}
Couple	0.608081	1.397961
Vertical force	1.699156	1.398312
Horizontal force	1.710820	1.421658

Table 2. Slope of the lines which minimizes the sum of the square of the errors of the respective data.
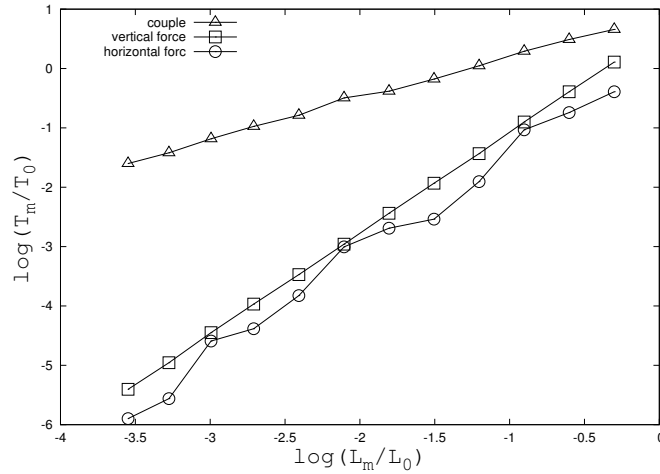
Figure 9. The normalized period $\log(T_k/T_0)$ versus the normalized horizontal projection of the length of the curve $\log(L_k/L_0)$ for 14 samples obtained from the eighth order term of the mixed triadic-quadratic Koch sequence, with $b = 1/2$.

dynamical fractal dimension should give $D_{\mathrm{approx}} = 2D_{\mathrm{dyn}}$ for the case of excitation induced by a moment and $D_{\mathrm{approx}} = 2(D_{\mathrm{dyn}} - 1)$ for the case of excitation induced by a horizontal or vertical force. The interpolated straight lines were adjusted to fit the point sets $\{T_k/T_0, L_k/L_0\}$ displayed on the Figure 6 with the least mean square deviation method.

The mass was assumed constant for all oscillators. As shown in the Table 2 the maximum error obtained with this technique is less than 3% and corresponds to the horizontal excitation. Clearly the points corresponding to the horizontal excitation presents a large dispersion. For excitations corresponding to a couple or a vertical force the errors do not exceed 1.2%.

3.3. *Random mixed structures.* It has been shown that the dynamical approach provides very good and consistent results for regular, deterministic curves belonging to the Koch family. The method has also proved to be successful in determining the fractal characteristics of mixed fractal curves.

For the classical Koch curves, besides providing means to determine the classical fractal dimension, the dynamical approach tell us if the geometry is random or not. For the regular generation process, the n-th order term is obtained from the $(n-1)$-th term following a well determined rule. What we call random geometry is that one obtained in a similar way except that the regular rule is replaced by a random orientation procedure.
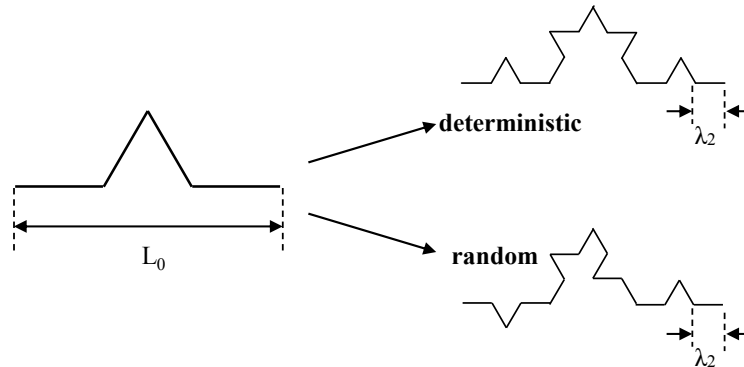
Figure 10. The first two terms of two Koch triadic curves: the classical deterministic curve (top) and a random generation (bottom). Both have the same Hausdorff dimension.

Figure 10 illustrates what we mean by a random fractal, taking as an example the classical Koch triadic. Note that the cover set for both curves is the same and therefore they have the same Hausdorff dimension. However note that the random series doesn't present the self-similarity property. Also, if the box counting technique were applied to compute the fractal dimension of these curves the results would be the same for all curves. The dynamical approach however is able to identify the random character of the curve.

Consider four terms of the triadic-quadratic odd series O^{odd} corresponding to five different random generations. Consider the corresponding simple oscillators excited by a horizontal force. The results correlating the normalized periods T_k/T_0 and the relative lengths λ_k/L_0 are displayed in Figure 11. The curves obtained by connecting the point set $\{T_k/T_0, \lambda_k/L_0\}$ for each random series clearly do not coincide. However similar construction connecting the point set derived from the excitation induced by
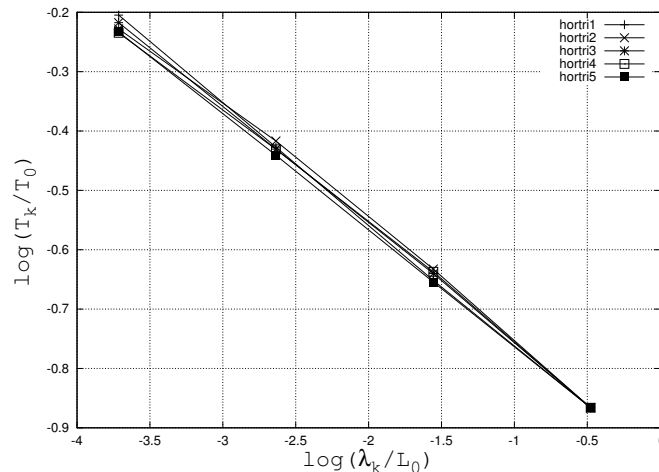
Figure 11. Logarithm of the normalized period versus the logarithm of the relative length of the elementary segment for five random triadic-quadratic sequences taking only odd iterations with initial conditions induced by a horizontal force.

a concentrated moment would lead to just one and the same curve. The reason is that for this particular type of excitation, that is, a concentrated moment, the strain energy is uniformly distributed along the curve which is the dynamical equivalent to the set covering introduced in the Hausdorff theory [Falconer 1990].

Indeed, recall that we are considering only the elastic energy induced by the bending moment. For the case of a moment this energy is independent of the orientation of the segments in the oscillator and consequently the results are the same for all random curves of the same order k. Now for excitations due to a horizontal or a vertical force the bending moment distribution depends on the position of each segment in the oscillator. This indicates that the elastic energy stored in the oscillator is sensitive to the position of the segments in the structure and this is translated in the point set distribution identifying the randomness of the structure formation. The slopes of the interpolated straight lines representing the points $\{T_k/T_0, L_k/L_0\}$ for each random series lead as expected to a unique value related closely to the Hausdorff dimension. That is on the average the result coincides with the other classical methods but the slight dispersion of the points reveals the random character of the series.

4. Conclusions

The technique proposed in a series of papers [Bevilacqua and Barros 2007; Bevilacqua et al. 2008] is applied here to mixed structures. The results reproduce the expected output of the method. All the experiments lead to the conclusion that this method is powerful and justify further exploration, encompassing both theoretical and computational fields. What the method suggests is that the dynamical properties of fractal, self-similar structures and random structures hide very rich information that need to be further investigated. In order to detect details as that associated to multi-fractals structures, random formation, mixed fractals and the like it would be convenient to use more complex oscillators for the identification problem with several added masses, that is extend the method to multi-mass systems. Possibly the frequency spectrum of those more complex structures will provide the information needed for the corresponding characterization. Application can be found in the determination of fractal dimension, if any, of protein chains, tissues and biological membranes [Bassingthwaighte et al. 1994]. It is also important to remark that this technique can be applied to physical objects, that is, characterization through laboratory experimentation. Therefore laboratory experiments can be designed to determine the dynamical properties of biological tissues or fibers and consequently the fractal characterization of the sample. The fractal characterization of composite materials may also be obtained using samples of the material to be analyzed and applying the procedure described above.

In [Bassingthwaighte et al. 1994, Chapter 12] the question is raised of "*fractals where the physical mechanism must be different at different scales*", referring to problems related to neural networks. The analysis introduced here may give some clues to explain this kind of puzzling behavior. Indeed if the mechanical properties of the oscillators are different at different scales then the sequence of periods of the oscillators may follow a power law quite different from that characterizing the geometric sequence, or even not be fractal at all. This means that for the general case the physical behavior may generate a sequence of physical properties quite different from the geometric characteristics.
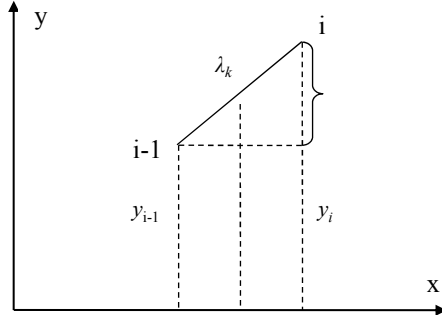
Figure 12. Mean value $\bar{y}_{i-1 \cdot i}$ and difference $\Delta y_{i-1,i}$.

Finally we would like to remark the interesting property of mixed fractals formed by two Koch curves that split up into two different sets. One is fractal and the other is quasifractal. To the best of our knowledge this is a new result that needs further investigation and generalization for structures constructed with more than two Koch curves.

Appendix

We show that the first derivative of the bilinear term Ω_k with respect to λ_k is finite for increasing values of k. Recall that

$$\Omega_k = \frac{1}{N_k} \sum_{i=0}^{N_k} \alpha_i(k) \quad \text{and} \quad \alpha_i(k) = \tfrac{1}{3}[z_{i-1}^2 + z_{i-1}z_i + z_i^2].$$

First let us write $\alpha_i(k)$ under the form

$$\alpha_i(k) = \bar{z}_{i-1,i}^2 + \tfrac{1}{3}\Delta z_{i-1,i}^2, \tag{17}$$

where

$$\bar{z}_{i-1,i} = (z_{i-1} + z_i)/2 \quad \text{and} \quad \Delta z_{i-1.i} = (z_i - z_{i-1})/2.$$

Introducing (17) in the expression for Ω_k we get

$$\Omega_k = \frac{1}{N_k} \sum_{i=0}^{N_k} (\bar{z}_{i-1,i}^2 + \tfrac{1}{3}\Delta z_{i-1,i}^2). \tag{18}$$

Clearly $\bar{z}_i \leq 1$ and $|\Delta z_{i-1,i}| \leq 1$.

Consider the second term on the right-hand side of (18). By definition $\Delta y_{i-1,i} = y_i - y_{i-1}$ as shown in Figure 12 and therefore it is possible to write

$$\Delta y_{i-1,i} = \gamma_{i-1,i}\lambda_k \quad \text{with} \quad \gamma_{i-1,i} \leq 1.$$

From this it follows that

$$\Delta z_{i-1,i} = \frac{1}{2h_0}\Delta y_{i-1,i} = \frac{1}{2h_0}\gamma_{i-1,i}\lambda_k = \beta_{i-1,i}\lambda_k.$$

Introducing this expression in (18) we get

$$\Omega_k = \frac{1}{N_k} \sum_{i=0}^{N_k} (\bar{z}_{i-1,i}^2 + \tfrac{1}{3}\beta_{i-1,i}^2 \lambda_k^2). \tag{19}$$

Now define the vector functions

$$\bar{z}_k^T = \left[\bar{z}_{0,1}^{(k)} \bar{z}_{1,2}^{(k)} \cdots \bar{z}_{i-1,i}^{(k)} \cdots \bar{z}_{N_k-1,N_k}^{(k)}\right]$$

and

$$\boldsymbol{\beta}_k^T = \frac{1}{2\sqrt{3}h_0} \left[\beta_{0,1}^{(k)} \beta_{1,2}^{(k)} \cdots \beta_{i-1,i}^{(k)} \cdots \beta_{N_k-1,N_k}^{(k)}\right].$$

Then (19) reads, in vector notation,

$$\Omega_k = \frac{1}{N_k} (z_k^T z_k + \lambda_k^2 \boldsymbol{\beta}_k^T \boldsymbol{\beta}_k).$$

Since $|z_{i-1,i}| \le 1$, $|\beta_{i-1,i}| \le 1$ and $\lambda_k \le M$ for all k, we conclude that Ω_k remains bounded as $k \to \infty$. Similarly the term of order $k+1$ can be written as

$$\Omega_{k+1} = \frac{1}{N_{k+1}} \left(\bar{z}_{k+1}^T \bar{z}_{k+1} + \tfrac{1}{3}\lambda_{k+1}^2 \boldsymbol{\beta}_{k+1}^T \boldsymbol{\beta}_{k+1}\right),$$

where the components of z_{k+1} are proportional to the ordinates of the corners of the curve corresponding to the term of order $k+1$. In general we may write

$$z_{k+1}^T = \frac{1}{h_0} \left[y_0^{(k+1)} y_1^{(k+1)} y_2^{(k+1)} \cdots y_{N_k+1}^{(k+1)}\right].$$

Referring to the preceding term in the sequence as shown in Figure 13 we have

$$z_{k+1}^T = \frac{1}{h_0} \left[y_0^{(k)} y_{01}^{(k)} \cdots y_{0(p-1)}^{(k)} y_1^{(k)} \cdots y_{1(p-1)}^{(k)} \cdots y_{N_k}^{(k)}\right]$$

Note that

$$y_{N_k}^{(k)} = y_{pN_k}^{(k+1)},$$
$$y_i^{(k)} = y_{pi}^{(k+1)},$$
$$y_{ij}^{(k)} = y_{pi+j}^{(k+1)}, \quad i = 0, \ldots, N_k - 1; \; j = 1, \ldots, p-1$$

represent respectively the ordinates of the corners of the k-th curve in the sequence and the ordinates of the added corners for the $(k+1)$-th curve. It is possible then to decompose the vector z_{k+1} as

$$z_{k+1} = \frac{\boldsymbol{U}_1}{h_0} \left[y_0^{(k)} y_1^{(k)} \cdots y_{N_k}^{(k)}\right]^T + \frac{\boldsymbol{U}_2}{h_0} \left[y_{01}^{(k)} \cdots y_{0(p-1)}^{(k)} y_1^{(k)} \cdots y_{1(p-1)}^{(k)} \cdots y_{(N_k-1)(p-1)}^{(k)}\right],$$

where $\boldsymbol{U}_1$ and $\boldsymbol{U}_2$ are Boolean matrices.

Now, with this decomposition it is not difficult to show that the vector $\bar{z}_{k+1}$ can be written as

$$\bar{z}_{k+1} = \boldsymbol{R}\bar{z}_k + \boldsymbol{R}(\boldsymbol{\Delta}z_k) + \lambda_k \boldsymbol{\rho}_{k+1}, \quad \text{where } |\rho_i^{(k+1)}| \le 1$$
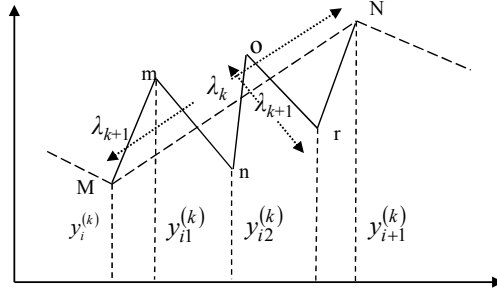
Figure 13. Term of order $k+1$ attached to the previous term of order k. $MN = \lambda_k Mm = mn = no = or = rN = \lambda_{k+1}$.

and $\boldsymbol{R} = [r_{ij}]$ is a Boolean matrix defined as follows (where i, j, p are integers):

$$r_{ij} = \begin{cases} 1 & \text{if } p(j-1) < i \le pj, \\ 0 & \text{otherwise.} \end{cases}$$

Now using the definition of Ω_{k+1} and recalling that $(\boldsymbol{\Delta z}_k) = \lambda_k \boldsymbol{\beta}_k$ we get

$$\Omega_{k+1} = \Omega_{k+1}^* + \frac{1}{3N_{k+1}} \lambda_{k+1}^2 \boldsymbol{\beta}_{k+1}^T \boldsymbol{\beta}_{k+1},$$

where

$$\Omega_{k+1}^* = \frac{1}{N_{k+1}} (\bar{\boldsymbol{z}}_k^T \boldsymbol{R}^T \boldsymbol{R} \bar{\boldsymbol{z}}_k + \lambda_k^2 \boldsymbol{\beta}_k^T \boldsymbol{R}^T \boldsymbol{R} \boldsymbol{\beta}_k)$$
$$+ \frac{2}{N_{k+1}} (\lambda_k \boldsymbol{\beta}_k^T \boldsymbol{R}^T \boldsymbol{R} \bar{\boldsymbol{z}}_k + \lambda_k \boldsymbol{\rho}_{k+1}^T \boldsymbol{R} \bar{\boldsymbol{z}}_k + \lambda_k^2 \boldsymbol{\rho}_{k+1}^T \boldsymbol{R} \boldsymbol{\beta}_k) + \frac{1}{N_{k+1}} (\lambda_k^2 \boldsymbol{\rho}_{k+1}^T \boldsymbol{\rho}_{k+1}).$$

Recalling that

$$|z_i^{(k)}| \le 1, \quad |\beta_i^{(k)}| \le 1, \quad |\beta_i^{(k+1)}| \le 1, \quad |\rho_i^{(k+1)}| \le 1, \quad N_{k+1} = pN_k, \quad \lambda_{k+1} = \lambda_k/q$$

and that $\boldsymbol{R}$ according to the definition above has the property $\boldsymbol{R}^T \boldsymbol{R} = p\boldsymbol{I}$ we arrive at

$$\Omega_{k+1} = \frac{1}{N_{k+1}} \left(p(\bar{\boldsymbol{z}}_k^T \bar{\boldsymbol{z}}_k + \tfrac{1}{3} \lambda_k^2 \boldsymbol{\beta}_k^T \boldsymbol{\beta}_k) \right) + \lambda_k R_1(k, k+1) + \lambda_k^2 R_2(k, k+1),$$

where $R_1(k, k+1)$ and $R_2(k, k+1)$ are finite for all k, $\max(R_1, R_2) < M$ (finite). Finally recalling that $N_{k+1} = pN_k$ we get

$$\Omega_{k+1} = \Omega_k + \lambda_k R_1(k, k+1) + \lambda_k^2 R_2(k, k+1).$$

Now noting that

$$\Delta \lambda_k = \lambda_{k+1} - \lambda_k = \lambda_k \left(\frac{1}{q} - 1 \right).$$

We may write

$$\frac{\Delta \Omega_k}{\Delta \lambda_k} = \left(\frac{1}{q} - 1 \right)^{-1} (R_1(k, k+1) + \lambda_k R_2(k, k+1)).$$

Lemma. *For curves belonging to the Koch family — the class of curves defined by $N_k = p^k$ and $\lambda_k/L_0 = 1/q^k$ — the first order differential form of the quadratic term Ω_k with respect to λ_k is finite for increasing values of k, or equivalently decreasing values of λ_k. That is, the limit*

$$\lim_{k\to\infty} (\Delta\Omega_k/\Delta\lambda_k) = \lim_{\lambda_k\to 0} (\Delta\Omega_k/\Delta\lambda_k)$$

is finite.

References

[Bassingthwaighte et al. 1994] J. B. Bassingthwaighte, L. S. Liebovitch, and B. J. West, *Fractal physiology*, Oxford University Press, 1994.

[Bevilacqua and Barros 2007] L. Bevilacqua and M. M. Barros, "Dynamical fractal dimension: direct and inverse problems", pp. 127–136 in *IUTAM Symposium on dynamics and control of nonlinear systems with uncertainty* (Nanjing, 2006), edited by H. Y. Hu and E. Kreuzer, Springer, Dordrecht, 2007.

[Bevilacqua et al. 2008] L. Bevilacqua, M. M. Barros, and A. C. N. R. Galeão, "Geometry, dynamics and fractals", *J. Brazilian Soc. Mech. Sci. Eng.* **30** (2008), 11–21.

[Falconer 1990] K. Falconer, *Fractal geometry*, Wiley, 1990.

[Feder 1988] J. Feder, *Fractals*, Plenum Press, New York and London, 1988.

[Gouyet 1996] J. F. Gouyet, *Physics and fractal structures*, Masson, Springer, New York, 1996.

[Mandelbrot 1982] B. Mandelbrot, *The fractal geometry of nature*, Freeman, N.Y., 1982.

[Mauroy et al. 2004] B. Mauroy, M. Filoche, E. R. Weibel, and B. Sapoval, "The optimal bronchial tree is dangerous", *Nature* **427** (2004), 633–636.

LUIZ BEVILACQUA: bevilacqua@coc.ufrj.br
COPPE, Universidade Federal do Rio de Janeiro, Centro de Tecnologia, Bloco B, s/ 101, Cidade Universitária, 21945-970 Rio de Janeiro, Brazil

MARCELO M. BARROS: barros@lncc.be
Laboratório Nacional de Computação Científica, Rua Getúlio Vargas, 333, 25651-075 Petropolis, Brazil